Ahmad A. Hasan [1]
Yahya M. Abbas [2]
Fouad T. Ibraheem [1]
Bushra A. Hasan [1]

[1] *Department of Physics, College of Science, University of Baghdad, Baghdad, IRAQ*
[2] *Department of Sciences, College of Basic Education, University of Wasit, Wasit, IRAQ*

Optical and Gas Sensor Properties of PAN:PPy:Gr Nanocomposites

Polyacrylonitrile:Polypyrole (PAN:PPy) undoped and doped with graphene Nano composites were synthesized using casting methods. Optical properties were utilized to describe the effect of composite ratio PAN/PPy as well as doping with Nanoscale graphene on the energy gap and the optical constants. PAN/PPy undoped and doped with Nanoscale graphene was used to detect gas nitrogen dioxide. In this article, the effect of mixing PAN with PPy at different weight ratios without addition and with the addition of 2% nanoscale graphene to the previous mixture on gas sensing performance on a large scale is explored. The results showed that doping with graphene enhanced the performance of gas sensing properties. Moreover, the article which focused on the effect of doping with graphene on the sensitivity, response and recovery time of gas was also reviewed.

Keywords: PAN:Ppy; Optical properties; Gas sensing; Graphene
Received: 02 December 2023; **Revised:** 11 January 2024; **Accepted:** 18 January 2024

1. Introduction

Polyacrylonitrile (PAN) has a semi-crystalline structure and has the chemical formula $(C_3H_3N)_n$. It has a nitrile (CN) functional group connected to the polyethylene backbone as the unit structure. PAN introduces antecedents in a variety of technological fields, such as manufacturing carbon fibers, sensor materials, and composite reinforcement, or delivering drugs to wound dressings, respectively [1-2]. Optical techniques have provided good methods for examining the characteristics of semiconductors, particularly estimation of the absorption coefficient at different wavelengths, which gives vital knowledge on the material's band gaps. The sort of nature of the bonding system and the number of atoms can both be inferred from the difference in energy between orbitals. It is necessary to have knowledge of the band gabs in order to comprehend the electrical properties of the materials and assess the practical advantage. It is possible to control the refractive index's goal [3]. Due to its numerous special characteristics, including low actuation voltage, high conductivity (it is a conducting polymer), and biocompatibility, PPy is extensively studied [4-7]. For an electrochemical actuation, PPy has the greatest stroke value out of all conducting polymers [8]. PPy actuators have been fabricated by different techniques like: Electrodeposition [9], drop casting and electrospinning which provides very rapid formation of the nanofiber structure, high material elongation rate and a cross-sectional area reduction [10-11]. PPy is insoluble thus it cannot be electro spun and usually used with co-polymers like (PEO), PAN, polyvinylidene difluoride (PVDF) and polystyrene (PS) [12-14]. PAN/CNT electrospun nanofibers were created by Ju et al. [15] and coated with PPy using in situ chemical polymerization. Yong et al. [16] prepared Polyacrylonitrile/metal oxide nanofibrous mat by electrospining to detect gases. PAN/NiO composite fibers obtained by electrospinning by Kaidar et al. [17] using in gas sensitive materials. Graphene (Gr) has been investigated as a gas sensing material for almost 20 years due to its special characteristics like a high surface-to-volume ratio and carrier mobility. The graphene resistance can vary noticeably when one gas molecule is adsorbed, indicating the single-molecule level of sensing ability [18-21]. In 2007, Schedin et al. [22] first demonstrated the detection of a single NO_2 molecule by using pristine graphene in pure He or NO_2 at ambient pressure. Their findings also showed that the pristine Gr sensor responds to NH_3, CO, and H_2O in addition to NO_2. The detection of NH_3, CO, O_2, NO_2, H_2, CH_4, SO_2, H_2S, and volatile organic compounds (VOCs) was later done extensively using Gr-based sensors [23-28]. By using chemical vapor deposition (CVD-G), Yavari et al. [29] prepared a Gr sensor to concurrently detect the low concentration of NO_2 and NH_3. The detection limit for NO_2 and NH_3 gases, which are preferred by commercial sensors, respectively, reached 100 and 500 ppb. However, they must raise the temperature to 200°C in inert vapors in order to fully recover the pristine Gr sensors. According to Dan et al. [30], pristine Gr did not react to NH_3 at room temperature. The chemical inertness of virgin graphene was likewise predicted by the first-principles calculation [31]. These facts make it abundantly evident that in ambient conditions, pure graphene is nonselective and weakly binds to NH_3 molecules. As a result, the functionalization to produce particular linkages between pure Gr and NH_3 molecules is of interest. Metallic nanoparticles, metal oxides, organic molecules, or conducting polymers can all be used to functionalize graphene. In contrast, Graphene (Gr) is a technology that is shedding light on the horizon,

particularly in chemistry, physics, and materials science. Despite its recent development, Graphene has already revealed a wide range of its potential applications, including field emission, electronics, electrical properties energy, and sensor [32-33]. Doped polymers are intriguing research topics for theoretical and experimental studies because they have the physical and chemical characteristics needed for fixed applications.

The absorption and transmission spectra were recorded in wavelength range 200-1100 nm using a Shimadzu 1800 spectrophotometer to study the optical properties. All measurements were achieved at room temperature. The optical energy gap (E_g), absorption coefficient (α), refractive index (n), extinction coefficient (k), real (ε_r) and imaginary (ε_i) dielectric constants were calculated using the following relations:

$$\alpha = \frac{2.303A}{t} \quad (1)$$

$$(\alpha h\nu) = A(h\nu - Eg)^r \quad (2)$$

$$h\nu = \frac{1240}{\lambda(nm)} \quad (3)$$

$$n = \sqrt{\frac{4R}{(R-1)^2} - k^2} - \frac{(R+1)}{(R-1)} \quad (4)$$

$$k = \frac{\alpha\lambda}{4\pi} \quad (5)$$

$$\varepsilon_r = n^2 - k^2 \quad (6)$$

$$\varepsilon_i = 2nk \quad (7)$$

where A is constant, $h\nu$ is the energy of incident photon, r is the order of the optical transition according to the type of the electronic transition

The gas sensing measurements were carried out in air and in presence of NO_2 gas at different working temperatures (100,150 and 200°C). The following equations were used to calculate the sensitivity regarding the reducing and oxidizing gas sensors:

$$S = \frac{R_g - R_a}{R_a} \times 100\% \quad \text{if } R_g > R_a \quad (9)$$

$$S = \frac{R_a - R_g}{R_a} \times 100\% \quad \text{if } R_a > R_g \quad (10)$$

where R_a and R_g are the resistance in the presence of air and detected gas, respectively

This research concerned with PAN/PPy nanocomposited undoped and doped with Gr for NO_2 sensing. The article is composed from two parts the first is concerned with the optical properties, which describe the effect of composites ratio as well as doping on the optical energy gap and optical parameters. The second part summarize on the gas detection properties of PAN/PPy without and with adding 2% of nanographene at different temperatures. In the present work, we have carried out the UV-visible spectroscopy and measured the sensing properties of nanocomposites toward NO_2 gas.

2. Experimental details

Chemical polymerization was used to create polypyrrole. Merck provided the pyrrole monomer, which has a melting point of -24°C and a density of 0.97 g/cm^3 at 20°C. Acros Organics provided sodium dodecyl benzene sulfonate (DBSNa), a surfactant with an 88% purity level. From Qrec, iron(III) chloride hexahydrate ($FeCl_3.6H_2O$) was provided as an oxidant. The graphene (Gr) was supplied with a purity level of 98% and a diameter of 6 to 8 nm. BDH-England provided dimethyl sulfoxide (DMSO) with a purity level of 99.6%. A 3.48 g of DBSNa surfactant was dissolved in 100 cc of distilled water. Another container had 100 cc of pure water mixed with 27.03 g of the oxidant $FeCl_3.6H_2O$. In a 500 ml reaction flask, the solutions were combined and agitated for 15 minutes at two distinct temperatures, namely 0 and 28°C. The solution of 0.15 mol of pyrrole monomer was then dropped gradually into the mixture throughout the course of 240 minutes of reaction time. The resulted black PPy powder was filtered and washed with distilled water for several times. This powder was put in an oven for 8 hours at temperature of 60°C to be dried. The right amount of PAN and PPy are dissolved in 20 ml of DMF to execute the casting procedure. The mixture is then transferred to a plastic Petri dish after being swirled all night at room temperature. Nano Gr-doped composites were produced by adding 2% weight to them.

3. Results and Discussion

The UV-visible absorption spectra for PAN:PPy nanocomposites undoped and doped with a fixed ratio of Gr are shown in Fig. (1). The mixing ratios are 90/10, 85/15, and 80/20. All nanocomposites, except those undoped (80/20 PAN:PPy), exhibit two absorption peaks. The high intense peak at 350 nm is attributed to the electronic transition from the valance band, or highest occupied molecular orbital (HOMO), to the conduction band, or lowest unoccupied molecular orbital (LUMO), which corresponds to $\pi \rightarrow \pi^*$ band electronic transition of the benzenoid ring of PAN. The second type of transition, which is less intense, produces a peak in the wavelength range of 360-365 nm, which is ascribed to the polaron band $\rightarrow \pi^*$ band transition of the benzenoid ring to the quinonoid ring. The charge transfer between the benzenoid and quinonoid rings and the transition from the valance band to the conduction band are both associated with these peaks that absorb low energy and are attributed to free nonbonding electrons. These peaks match other researchers' findings quite well [34-35]. The red shift in the absorption peaks (shift to a longer wavelength) of undoped PAN:PPy (85/15) is caused by increasing the PPy ratio. This indicates a reduction of the optical band gap and is consistent with the findings of [36-37].

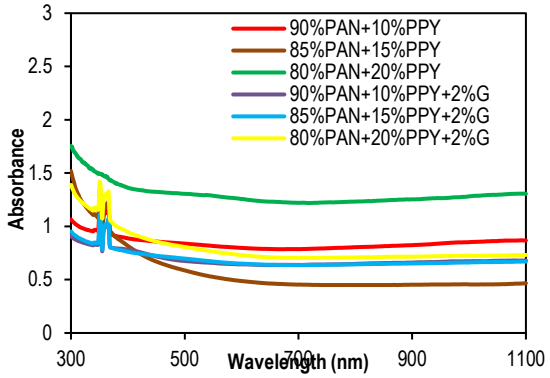

Fig. (1) The absorption spectra as a function of wavelength for (PAN /PPy) composites undoped and doped with 2 % graphene

The interaction between PPy molecules and the presence of hydrogen ions in the doped PAN may also cause the peak to shift. It is obvious that increasing the PPy ratio in composites causes the absorption to decrease, but as the PPy ratio is increased further, the opposite occurs in samples that have been doped with Gr, which causes the absorption to decrease due to the quantum size effect and results in a wide band gap (blue shift), as will be seen later. Figure (2) shows the optical transmission spectra of the undoped and Gr-doped PAN:PPy with various nanocomposites ratios. On the other hand, the transmittance increases as Gr is added to the composites because of a reduction in absorbance and a blue shift that occurs as a result of an increased quantum size effect. This is in accordance with [38-39]. The transmittance gets to change in a non-regular sequence, increasing and then decreasing. The chart makes it evident that the transmittance intensity increases as the wavelength increases, reaching a maximum value for undoped 85/15 PAN:PPy before decreasing.

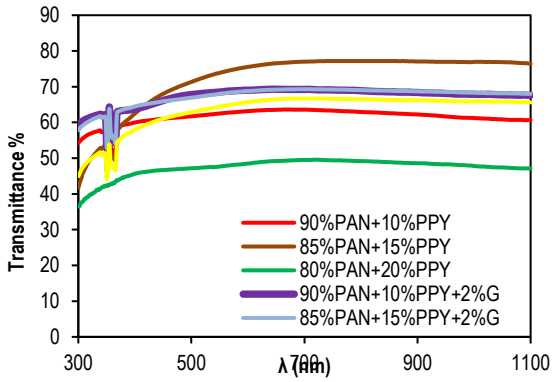

Fig. (2) The transmission spectra as a function of wavelength for (PAN /PPy) compositesundoped and doped with 2 % graphene

Since the development of covalent connections between polymer chains and additives decreased transmission at high energy, this behaviour was attributed to the interaction of additives. The electrons in the outer orbits moved to higher energy levels where there were open energy band spots. As a result, some of the incident light is not transmitted through it. Thus, the loss of dispersed light decreased as transmittance decreased and PPy content increased in the blend. In order to determine the energy gap, the plot of $(\alpha h\upsilon)^2$ as a function of photon energy was plotted as shown in Fig. (3), From this figure and table (1), it is clear that the energy gap is for a direct allowed transition since r=0.5. The optical energy gap showed a drastic reduction from 3.3 to 2.6 eV by increasing the PPy ratio from 10 to 20% in composite samples [5]. Tanski et al. calculated that the E_g for PAN, which was about 3.92 eV, indicated the dielectric nature of this material [40]. While the growth of the energy gap is attributed to the modification of polymer chains. The reduction of the energy gap is related to the narrow energy gap of PPY (2.1eV). This is attributed to the doping with graphene returning the energy gap to its original value of 3.3 eV, referred to as the quantum size effect.

The optical constants that imply refractive index, extinction coefficient, and real and imaginary dielectric constants are listed in table (1). The measured values at selected wavelengths (550 nm) for PAN/PPy nanocomposites are undoped and doped with 2% Gr. It is obvious that *n* reaches its minimum value as the PPy ratio increases from 10% to 15%, while it attains its maximum value by increasing PPy to 20% and then proceeding with a reduction in the *n* values of nanocomposites samples by doping with Gr. The reduction of *n* values can be explained by the fact that the increasing PPy ratio fastens the velocity of incident light (the material becomes more transparent), which in turn reduces the value of refractive index since it represents the ratio of the velocity of light in a vacuum to the velocity of light in the material, while the growth of *n* values is related to the reduction of the velocity of light (the material becomes more opaque) [41,42]. The behavior of *k* as a function of wavelength of (PAN/PPy) nanocomposites undoped and doped with 2% Gr is similar to that of *n*. The reduction of *k* values is related to the reduction of the absorption coefficient, while the growth of *k* values is related to high absorption values and an increase in the absorbed part of the incident light (direct relation between *k* and α). The behavior of real and imaginary dielectric constants of (PAN/PPy) nanocomposites undoped and doped with 2% Gr is shown in table (1). The same observation given for *n* and *k* can be used to explain the variation trend of ε_r and ε_i.

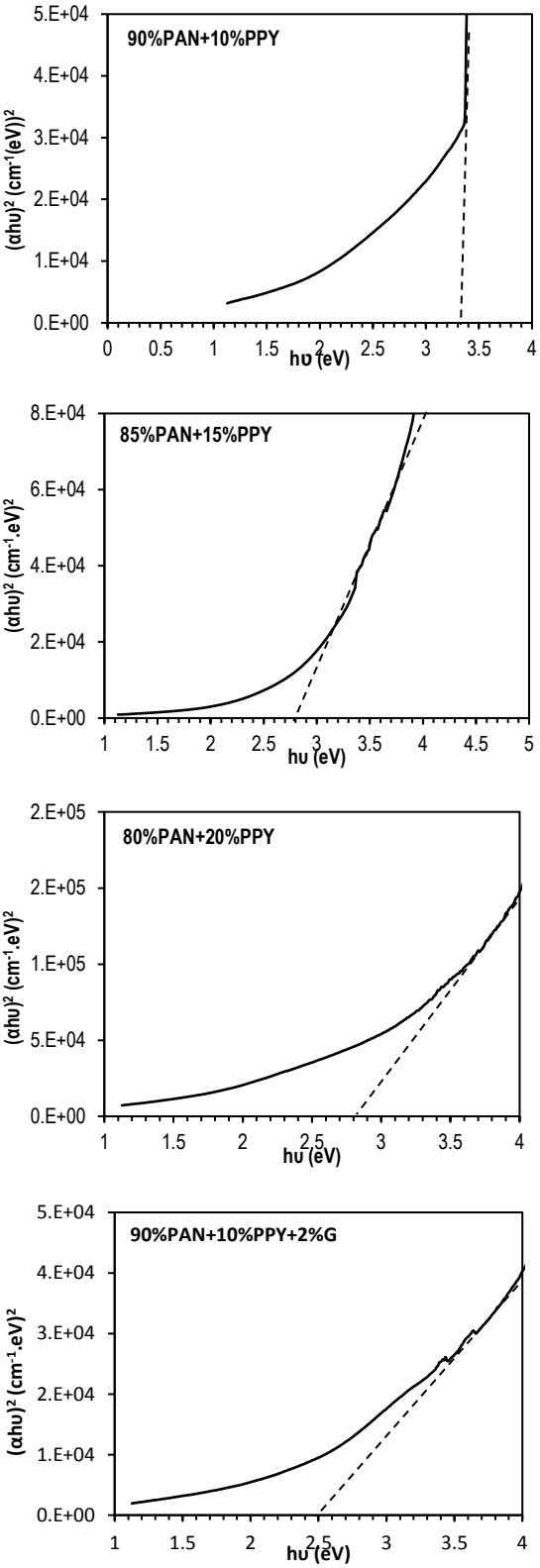

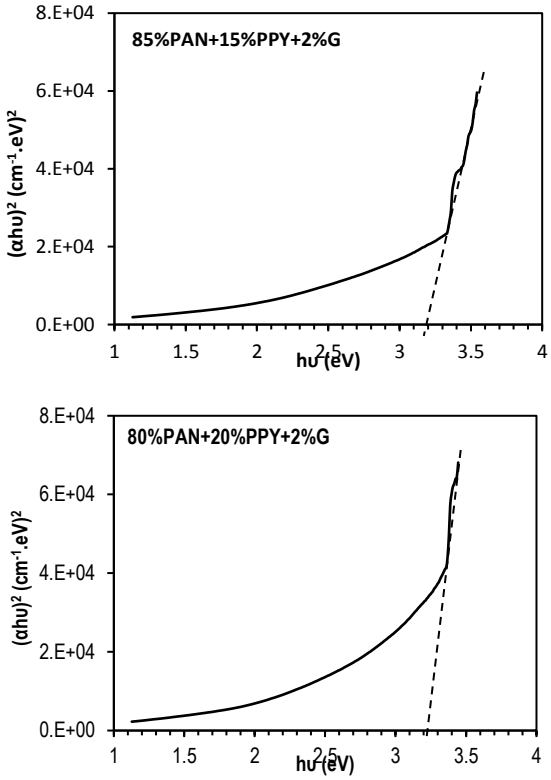

Fig. (3) Variation of $(\alpha h\nu)^2$ with photon energy (hv) for PAN/PPy nanocomposites undoped and doped with 2% grapheme

The plot of response time of (PAN/PPy) composites undoped and doped with graphene at different temperatures (100, 150 and 200°C) are shown in figures (4-9). The measured values of sensitivity, response and recovery times of the gas sensor at different temperatures in the presence of NO_2 are illustrated in table (2). The most noticeable remark from these figures, the resistance decreases of most sensors samples except (PAN/PPy 90/10 at 150°C and PAN/PPy 80/20 doped with Gr at all temperatures) in presence of the detected gas, while the resistance return to increase when the gas exposure is stopped. This behavior reflects the p-type nature of sensor as a result of semiconducting nature [43,44]. It is well-known that PAN and PPy are p-type semiconductors and the exposure to NO_2 oxidizing gas causes an increase in the conductance or reduction in the resistance. It is obvious sensitivity reduces with rising temperatures for low PPy ratio while the sensitivity grow up with increasing temperature for composites with high PPy ratio. On the other hand the sensitivity reach maximum value (91.53%) by doping 90%PAN/10%PPY composite with Gr. This is attributed to the fact that Gr added many sites with Gr that increase of PPy in composites samples which is responsible about the enhancement of hopping process in the composites samples [45-47].

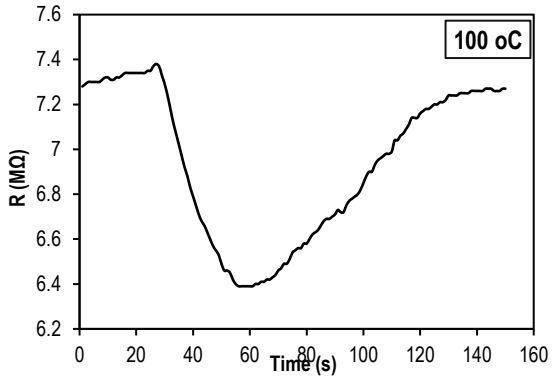

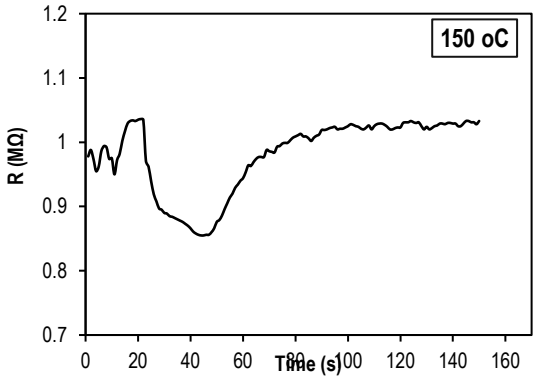

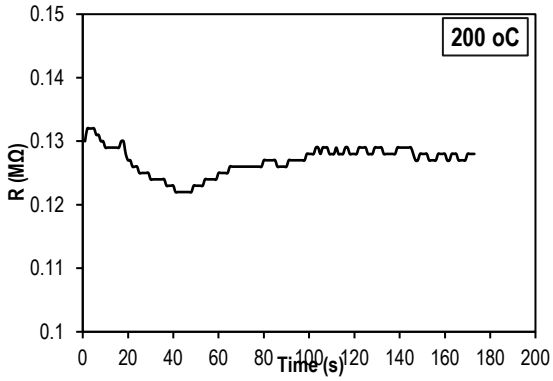

Fig. (4) The relation between the resistance and time for (90%PAN/10%PPy) nanocomposites

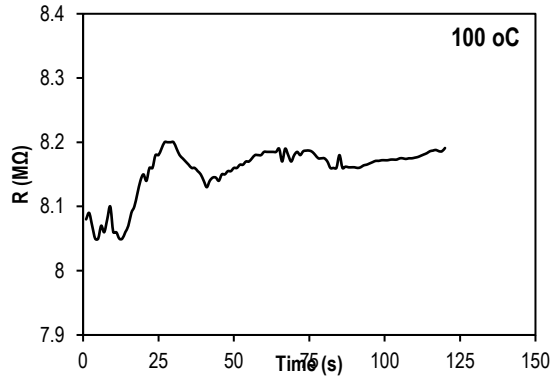

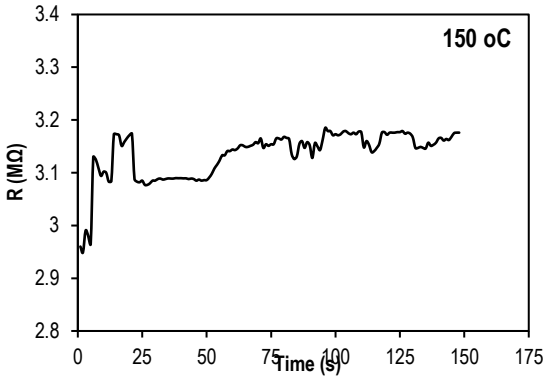

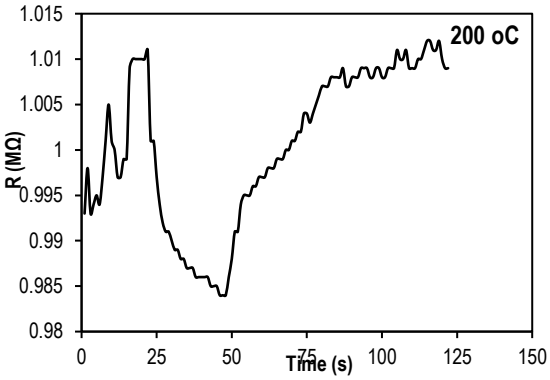

Fig. (5) The relation between the resistance and time for (85%PAN/15%PPy) nanocomposites

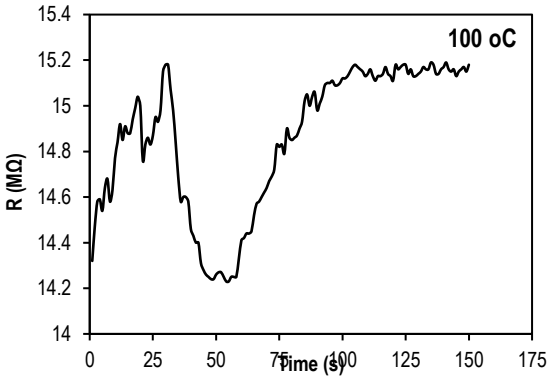

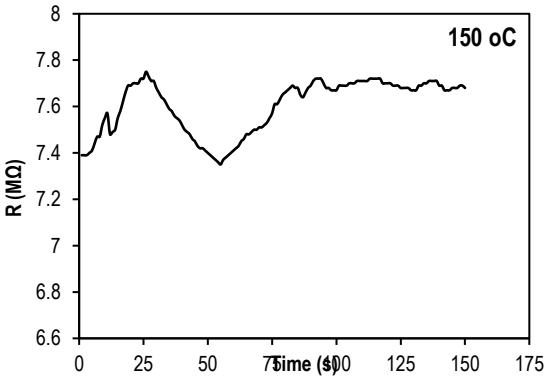

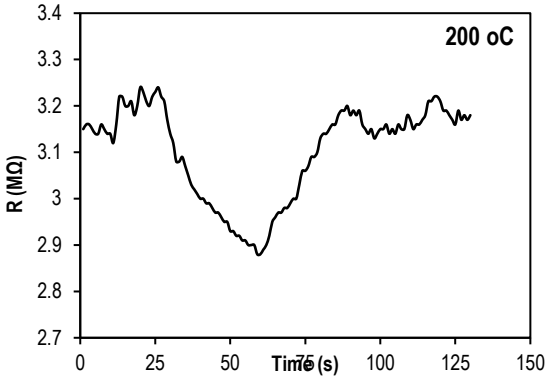

Fig. (6) The relation between the resistance and time for (80%PAN/20%PPy) nanocomposites

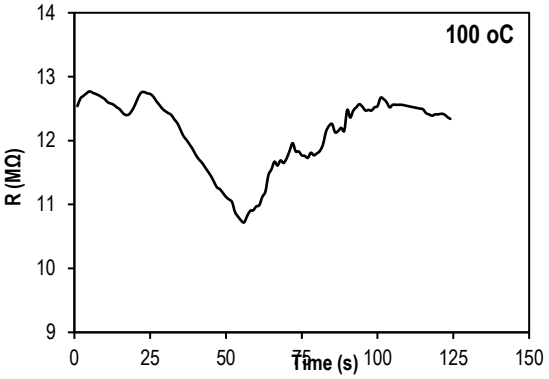

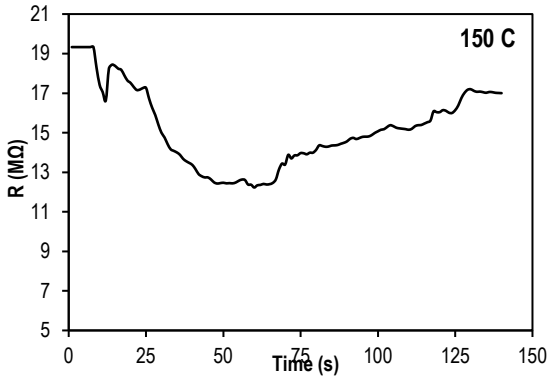

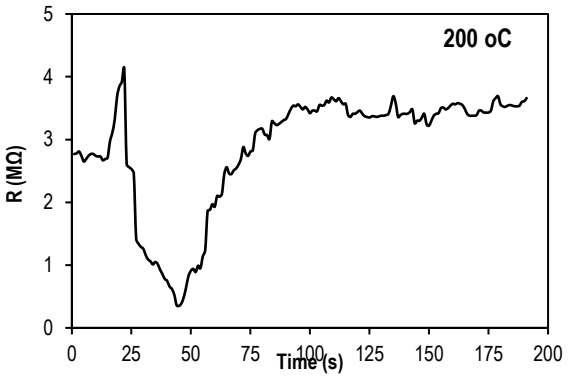

Fig. (7) The relation between the resistance and time for (90%PAN/10%PPy) nanocomposites doped with 2% Gr

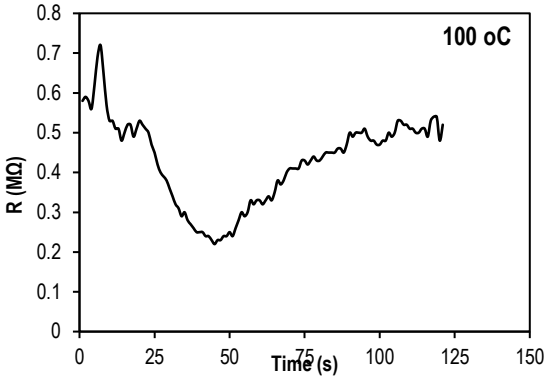

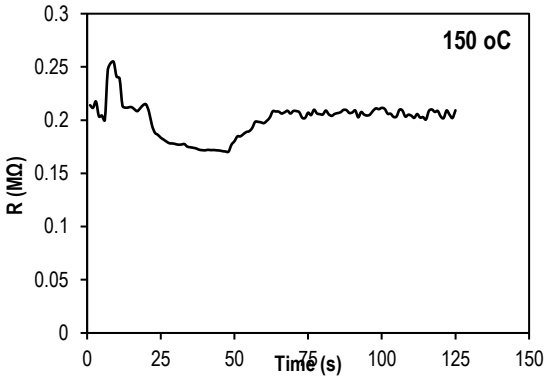

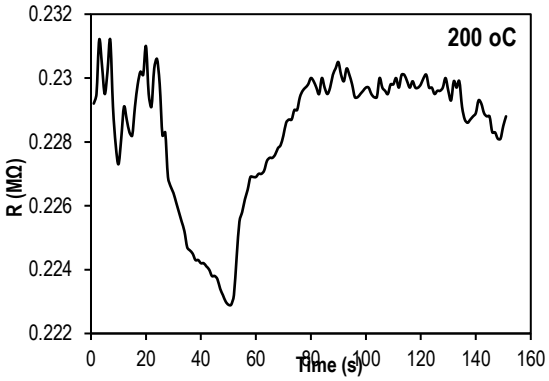

Fig. (8) The relation between the resistance and time for (85%PAN/15%PPy) nanocomposites doped with 2% Gr

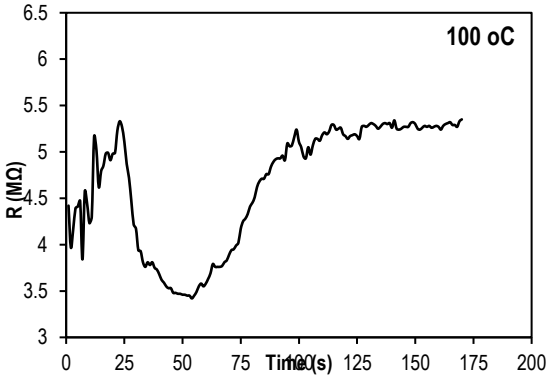

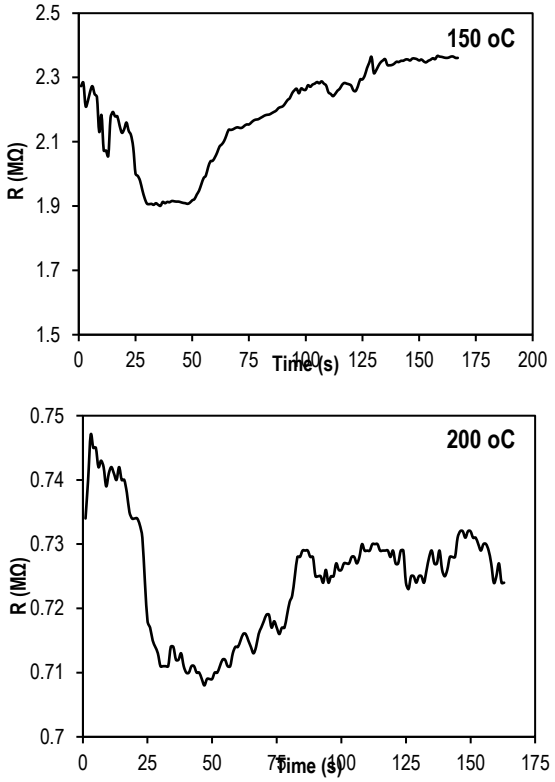

Fig. (9) The relation between the resistance and time for (80%PAN/20%PPy) nanocomposites doped with 2% Gr

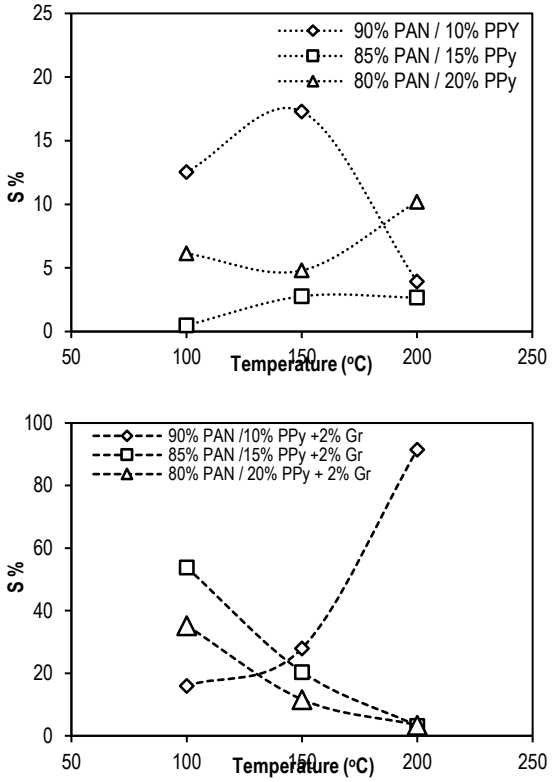

Fig. (10) The sensitivity (S) as a function of working temperature of PAN/PPy nanocomposites undoped and doped with 2% Gr

The relationship between the sensitivity and temperature change is depicted in Fig. (10), which suggests that the samples that were not doped with graphene did not exhibit consistent behaviour with temperature changes. Conversely, the samples that were doped with graphene exhibited consistent behaviour for each sample; the sample (90/10 PAN/PPy) increased in sensitivity as the temperature increased, while the other two samples decreased in sensitivity. Adsorption is the fundamental surface-related process, and surface area and material grain size are two important determinants of adsorption on the sensor's surface. Grain size reduction will result in an increase in surface area and better gas sensor characteristics. This is the region where sensors' sensitivity to gases is highest. Thus, as the surface to volume ratio rises, the sensor membrane's grain size may have a nanoscale size. Consequently, the majority of research focuses on producing semiconductor thin film sensors (nano). Grain size decrease causes grain boundaries to widen, increasing the adsorption surface area and contact, which raises response time and sensitivity value [48]. With varying particle sizes ranging from 5 to 80 nm, the researcher Rothschild et al. investigated the impact of particle size on the sensitivity of chemically resistant nano-gas sensors using the effective carrier concentration as a function of the surface-state density of the SnO_2 sensor material [49].

4. Conclusions

Nanocomposites from PAN/PPy undoped and doped with Gr were synthesized via casting method, while PPy were fabricated using chemical polymerization. The optical energy gap showed non regular reduction by increasing of PPy while it tend to increase by doping with Gr. The optical constants together get to change with variation of PPy ratio as well as by doping with Gr. The prepared gas sensors showed best performance for 90/10 and 80/20 PAN/PPy doped with Gr towards oxidizing gas. The temperature change did not show a consistent behavior on the sensitivity of the tested samples towards the gas used, as it fluctuated between increase and decrease for each sample.

References

[1] D.W Chae and B.Ch. Kim, "Effects of zinc oxide nanoparticles on the physical properties of polyacrylonitrile", *J. Appl. Polym. Sci.*, 99 (2006) 1854-1858.

[2] M.R. Almafie et al., "Dielectric Properties and Flexibility of Polyacrylonitrile/Graphene Oxide Composite Nanofibers", *Amer. Chem. Soc. Omega.*, 7 (2022) 33087-3309.

[3] P.K. Tien, R. Ulrich and R.J. Martin, "Optical second harmonic generation in form of coherent cerenkov radiation from a thin-film waveguide", *Appl. Phys. Lett.*, 17(10) (1970) 447-450.

[4] D. Kai et al., "Polypyrrole-contained electrospun conductive nanofibrous membranes for cardiac tissue

engineering", *J. Biomed. Mater. Res. A*, 99(3) (2011) 376-385.
[5] J.Y. Lee et al., "Polypyrrole-coated electrospun PLGA nanofibers for neural tissue applications", *Biomaterials*, 30(26) (2009) 4325-4335.
[6] J.D. Madden et al., "Artificial muscle technology: physical principles and naval prospects", *IEEE J. Ocean. Eng.*, 29(3) (2004) 706-728.
[7] L. Bay et al., "A conducting polymer artificial muscle with 12% linear strain", *Adv. Mater.*, 15(4) (2003) 310-313.
[8] S. Hara et al., "TFSI-doped polypyrrole actuator with 26% strain", *J. Mater. Chem.*, 14(10) (2004) 1516-1517.
[9] Y.M. Abbas and A.A. Hasan, "Optical Properties Study of Polypyrrole doped with TiO_2, WO_3, Fe_2O_3 and SnO_2 Nanoparticles", *IOP Conf. Ser.: Mater. Sci. Eng.*, 928 (2020) 072017.
[10] I.-H. Chen, C.-C. Wang and C.-Y. Chen, "Fabrication and structural characterization of polyacrylonitrile and carbon nanofibers containing plasma-modified carbon nanotubes by electrospinning", *J. Phys. Chem. C*, 114(32) (2010) 13532-13539.
[11] J.D. Madden et al., "Creep and cycle life in polypyrrole actuators", *Sens. Actuat. A: Phys.*, 133(1) (2007) 210-217.
[12] W. Zheng et al., "Artificial muscles based on polypyrrole/carbon nanotube laminates", *Adv. Mater.*, 23(26) (2011) 2966-2970.
[13] I.S. Chronakis, S. Grapenson and A. Jakob, "Conductive polypyrrole nanofibers via electrospinning: electrical and morphological properties", *Polymer*, 47(5) (2006) 1597-1603.
[14] J. Doshi and D.H. Reneker, "Electrospinning process and applications of electrospun fibers", *J. Electrostat.*, 35(2-3) (1995) 151-160.
[15] Y.-W. Ju et al., "Electrochemical properties of electrospun PAN/MWCNT carbon nanofibers electrodes coated with polypyrrole", *Electrochimica Acta*, 53(19) (2008) 5796-5803.
[16] D.Y. Lee, J.-E. Cho and Y.-J. Oh, "Gas Sensing properties of Polyacrylonitrile/metal oxide nanofibrous mat prepared by electrospining", *J. Korean Sens. Soc.*, 17 (2008) 281-288.
[17] B. Kaidar et al., "Gas Sensitive Materials Based on Polyacrylonitrile Fibers and Nickel Oxide Nanoparticles", *J. Compos. Sci.*, 6 (2022) 326.
[18] S. Nair, S. Natarajan and S.H. Kim, "Fabrication of electrically conducting polypyrrole-poly (ethylene oxide) composite nanofibers", *Macromol. Rapid Commun.*, 26(20) (2005) 1599-1603.
[19] X. Li et al., "Fabrication of Polyacrylonitrile/polypyrrole (PAN/PPy) composite nanofibres and nanospheres with core–shell structures by electrospinning", *Mater. Lett.*, 62 (2008) 1155-1158.
[20] R. Bogue and R. Graphene, "Sensors: A Review of Recent Developments", *Sens. Rev.*, 34 (2014) 233-238.
[21] K. Vikrant et al., "Materials as a Superior Platform for Advanced Sensing Strategies against Gaseous Ammonia", *J. Mater. Chem. A*, 6 (2018) 22391-22410.
[22] F. Schedin et al., "Detection of individual gas molecules adsorbed on grapheme", *Nat. Mater.*, 6 (2007) 652-655.
[23] C.W. Chen et al., "Oxygen sensors made by monolayer graphene under room temperature", *Appl. Phys. Lett.*, 99 (2011) 243502.
[24] J. Hong et al., "A Highly Sensitive Hydrogen Sensor with Gas Selectivity Using a PMMA Membrane-Coated Pd Nanoparticle/Single-Layer Graphene Hybrid", *ACS Appl. Mater. Interfaces*, 7 (2015) 3554-3561.
[25] Y. Kim et al., "Electrospun nanofibrous Polyacrylonitrile (PAN)/FeO_3 membrane as CO_2 gas sensor", *J. Korean Ceram. Soc.*, 44 (2007) 194-197.
[26] Y. Yoon et al., "Metal-Oxide Nanomaterials Synthesis and Applications in Flexible and Wearable Sensors", *Amer. Chem. Soc. Nanosci.*, 2 (2022) 64-92.
[27] P.A. Pandey, N.R. Wilson and J.A. Covington, "Pd-doped reduced graphene oxidesensing films for H_2 detection", *Sens. Actuat. B: Chem.*, 183 (2013) 478-487.
[28] L. Huang et al., "Multifunctional Graphene Sensors for Magnetic and Hydrogen Detection", *ACS Appl. Mater. Interfaces*, 7 (2015) 9581-9588.
[29] F. Yavari et al., "High sensitivity detection of NO_2 and NH3in air using chemical vapor deposition grown grapheme", *Appl. Phys. Lett.*, 100 (2012) 203120.
[30] Y. Dan et al., "Intrinsic Response of Graphene Vapor Sensors", *Nano Lett.*, 9 (2009) 1472-1475.
[31] D.S.L. Abergel et al., "Properties of graphene: A theoretical perspective", *Adv. Phys.*, 59 (2010) 261-482.
[32] S. Cetiner et al., "Polypyrrole / Polyacrylonitrile Composite Films :Dielectric, Spectrophotometric and Morphologic Characterization", *Fibers Polym.*, 11 (2010) 843-850.
[33] A.K. Geim, "Graphene: Status and Prospects", *Science*, 324 (2009) 1530-1534.
[34] S. Ameen, M.S. Akhtar and H.S. Shin, "Hydrazine chemical sensing by modified electrode based on in situ electrochemically synthesized polyaniline /graphene composite thin film", *Sens. Actuat. B: Chem.*, 173 (2012) 177-183.
[35] R.K.F. Alfahed et al., "Structural, morphological, and Z-scan technique for a temperature-controllable chemical reaction synthesis of zinc sulfide nanoparticles", *Appl. Phys. B, Lasers Opt.*, 48 (2019) 125.
[36] M.G. Cho, S.K. Oh and S.S. Im, "Preparation and characterization of polyaniline nanoparticles synthesized from DBSA micellar solution", *Synth. Met.*, 126 (2002) 53-60.
[37] C.M.H. Al-humairi, "Study the Optical and Electrical Properties of (PVA-Ag) and (PVA-TiO_2)

Nanocomposites", M.Sc. thesis, University of Babylon (2013).
[38] K.M. Ziadan, "The electronic transitions of polyaniline doped with p-toluene sulfonic acid", *1st Sci. Conf.*, College of Science, University of Basrah (2013).
[39] T. Tański, W. Matysiak and Ł. Krzemiński, "Analysis of Optical Properties of TiO_2 nanoparticles and PAN/TiO_2 composite nanofibers", *Mater. Manuf. Processes*, 32 (2017) 1-7.
[40] I.S. Chronakis, S. Grapenson and A. Jakob, "Conductive polypyrrole nanofibers via electrospinning: electrical and morphological properties", *Polymer*; 47(5) (2006) 1597-1603.
[41] B.A. Hasan et al., "Structural, Morphology and Optical Properties of Al_xSb_{1-x} Thin Films Prepared by Pulsed Laser Deposition (PLD)", *AIP Conf. Proc.*, 2372 (2021) 040010.
[42] S.S. Mahmood and B.A. Hasan, "Effect of Dopant Concentration on the Structural, Optical and Sensing Properties of $(SnO_2)_{1-x}(TiO_2:CuO)_x$ Sprayed Films", *Baghdad Sci. J.*, 16 (2019) 2.
[43] A. Gurlo et al., "A n- to p- conductivity transition induced by oxygen adsorption on α-Fe_2O_3", *Appl. Phys. Lett.*, 85 (2004) 2280-2282.
[44] P. Liu et al., "A Fast Response Ammonia Sensor Based on Coaxial PPy–PAN Nanofiber Yarn", *Nanomaterials*, 6 (2016) 121.
[45] Y.M. Abbas and A. Abbas, "Dielectric and gas sensing properties of *in situ* electrochemically polymerized PPy-MgO-WO_3 nanocomposite films", *Iraqi J. Sci.*, 62 (2021) 2915-2933.
[46] S. Dogan, L. Toppare and U. Akbulut, "Conducting polymers of Anilne: 1. Electrochemical Synthesis of a Conducting Composite", *Synth. Met.*, 53 (1992) 29-35.
[47] S. Dogan et al., "Conducting polymers of Anilne: 2. A Composite as a Gas sensor", *Synth. Met.*, 60 (1993) 27-30.
[48] G. Korotcenkov et al., "Gas sensing properties of SnO_2 thin films modified by Ag nanoclusters synthesized by SILD method", *Int. J. Mater. Metallur. Eng.*, 5 (2011)776-779.
[49] A. Rothschild and Y. Komem, "The effect of grain size on the sensitivity ofnanocrystalline metal oxide gas sensors", *J. Appl. Phys.*, 95 (2004) 6374-6380.

Table (1) The values of energy gap (E_g) ,n, k, ε_r and ε_i of (PAN/PPy) composites undoped and doped with 2 % graphene

Sample	T %	α (cm^{-1})	k	n	ε_r	ε_i	Eg (eV)
90%PAN+10%PPY	62.52	47	2.1E-04	2.409	5.803	9.9E-04	3.32
85%PAN+15%PPY	73.88	30	1.3E-04	2.126	4.520	5.6E-04	2.80
80%PAN+20%PPY	47.67	74	3.2E-04	2.629	6.913	1.7E-03	2.60
90%PAN+10%PPY+2%Gr	68.51	38	1.7E-04	2.269	5.147	7.5E-04	2.63
85%PAN+15%PPY+2%Gr	68.00	39	1.7E-04	2.282	5.205	7.7E-04	3.20
80%PAN+20%PPY+2%Gr	64.42	44	1.9E-04	2.367	5.603	9.1E-04	3.25

Table (2) Values of sensitivity, response and recovery time of PAN/PPy Nanocomposites undoped and doped with 2% Gr for NO_2 gas

Sample	Temperature (°C)	Sensitivity (%)	Response Time (s)	Recovery Time (s)
90%PAN/10%PPy	100	12.53	30.6	84.6
	150	17.29	22.5	47.7
	200	3.9	23.4	48.6
85%PAN/15%PPy	100	0.49	20.7	51.3
	150	2.77	26.1	45
	200	2.67	22.5	47.7
80%PAN/20%PPy	100	6.13	20.7	87.3
	150	4.8	27	58.5
	200	10.2	32	56.7
90%PAN/10%PPy+2%Gr	100	15.98	29.7	57.6
	150	28.00	26.1	45
	200	91.53	20.7	94.5
85%PAN/15%PPy+2%Gr	100	53.84	19.8	69.3
	150	20.41	25.2	46.8
	200	3.21	24.3	45
80%PAN/20%PPy+2%Gr	100	35.27	27	87.3
	150	11.62	23.4	92.7
	200	3.4	24.3	63

